Supporting Information for

Discovery of Novel Pim-1 Kinase Inhibitors with a Flexible-Receptor Docking Protocol

Gudong Li,[†,#] *Wei Li,*[*,‡,#] *Yuting Xie,*[‡] *Xiaobo Wan,*[‡] *Guojun Zheng,*[†] *Niu Huang,*[*,‡,§] *and Yu Zhou*[*,‡]

[†]State Key Laboratory of Chemical Resources Engineering, Beijing University of Chemical Technology, Beijing 100029, China.

[‡]National Institute of Biological Sciences, Beijing, No. 7 Science Park Road, Zhongguancun Life Science Park, Beijing, 102206, China.

[§]Tsinghua Institute of Multidisciplinary Biomedical Research, Tsinghua University, Beijing 102206, China.

[*]Correspondence. E-mail: zhouyu@nibs.ac.cn; huangniu@nibs.ac.cn.

Table of Contents

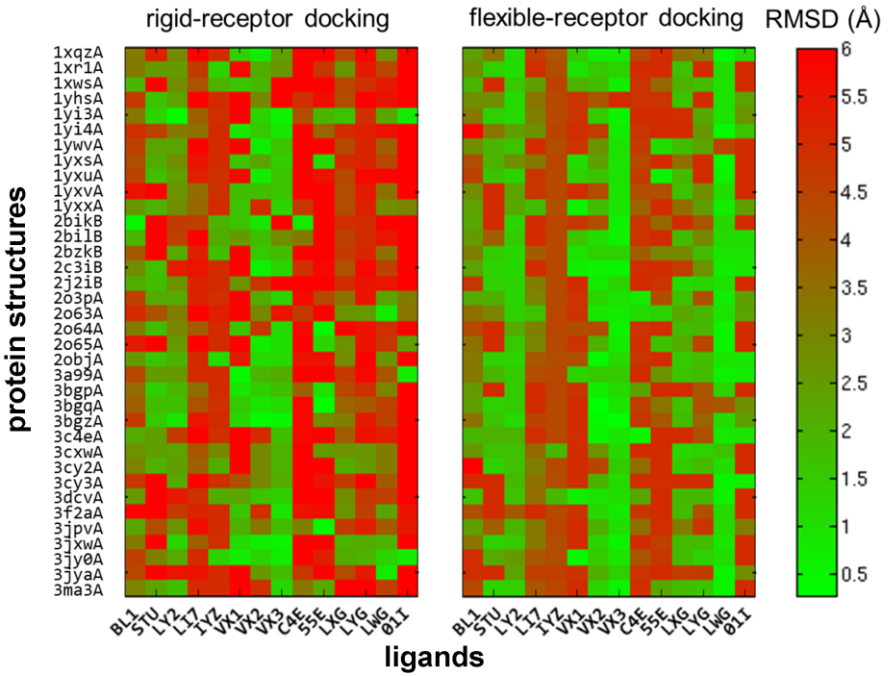

Figure S1. Pose fidelity in cross docking of crystal ligands of Pim-1 kinase. The ligand labels refer to their ligand ID from the Protein Data Bank (PDB).

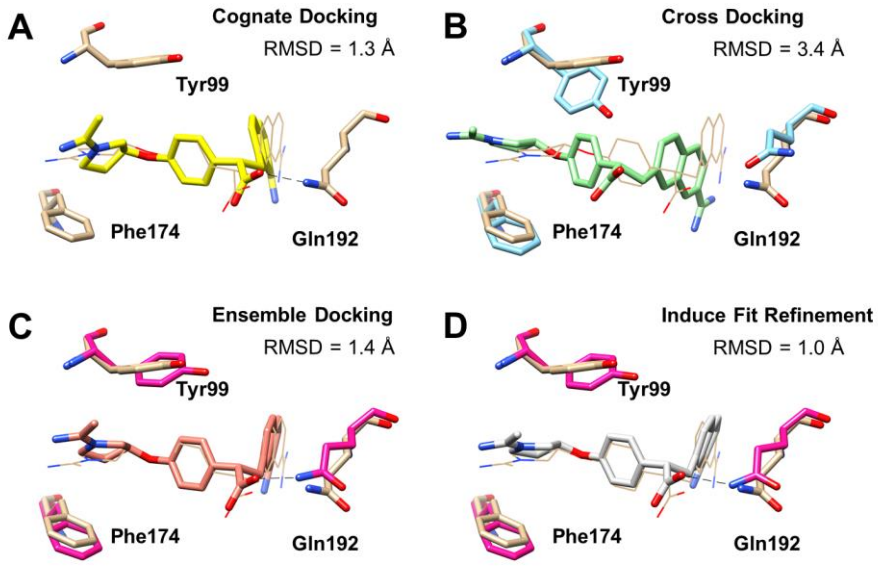

Figure S2. Binding pose prediction of DX9 against Factor Xa. (A) Rigid docking of DX9 into its cognate receptor (PDB ID: 1FAX). (B) Rigid cross docking of DX9 from 1FAX to 1KSN. (C) "Ensemble Docking" of DX9 from 1FAX to 1KSN. (D) "Induced Fit Refinement" of the complex generated by "Ensemble Docking".

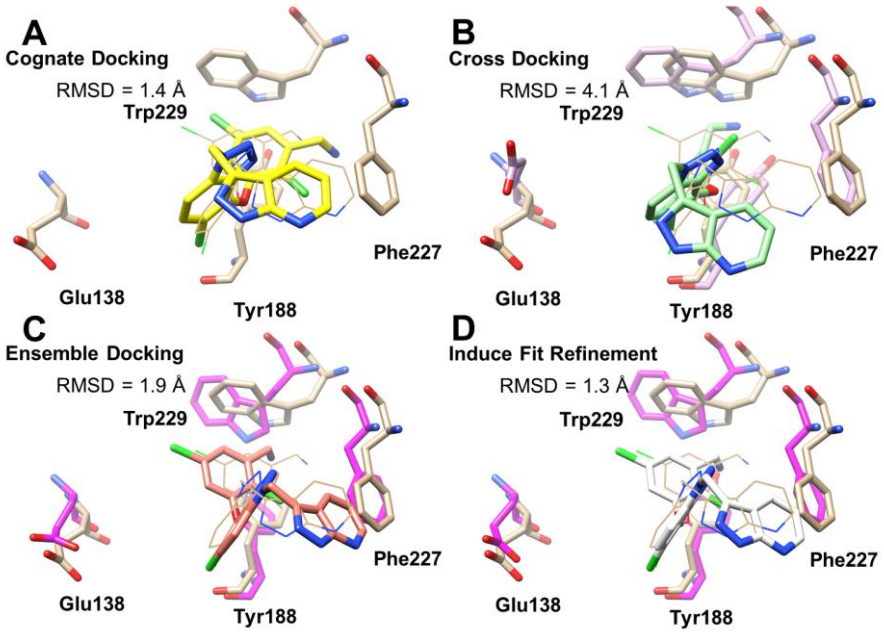

Figure S3. Binding pose prediction of 5MA against HIV-RT. (A) Rigid docking of 5MA into its cognate receptor (PDB ID: 3T19). (B) Rigid cross docking of 5MA from 3T19 to 1RTH. (C) "Ensemble Docking" of 5MA from 3T19 to 1RTH. (D) "Induced Fit Refinement" of the complex generated by "Ensemble Docking".

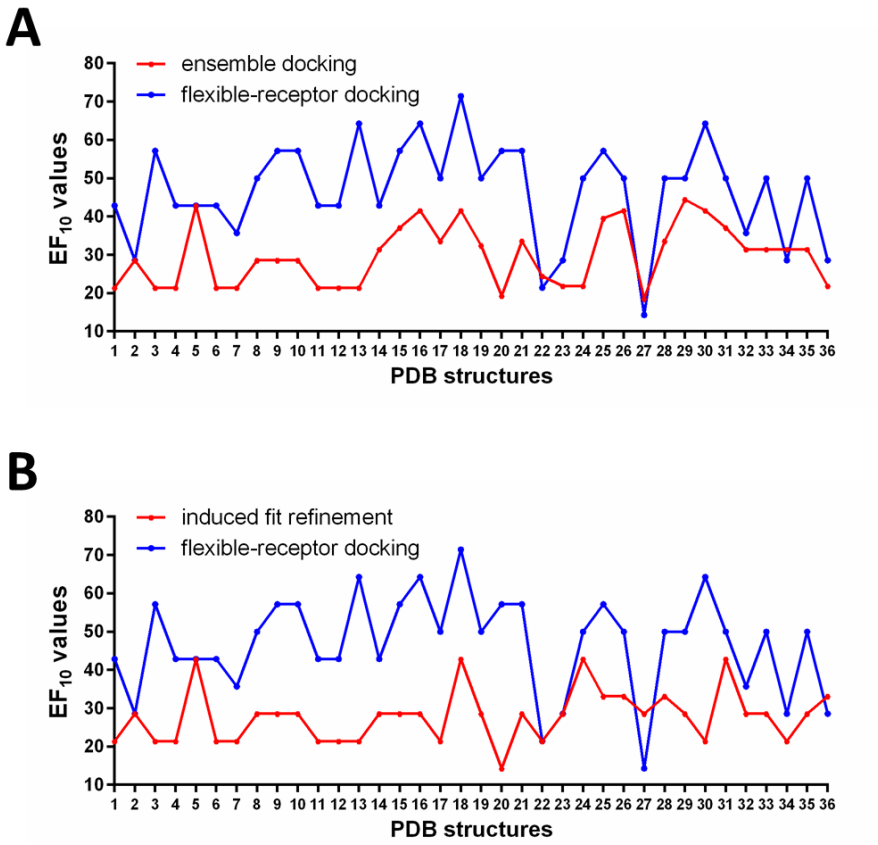

Figure S4. Enrichment performance in retrospective virtual screening of known Pim-1 kinase ligands. (A) Comparison of the flexible-receptor docking protocol with "Ensemble Docking" approach. (B) Comparison of the flexible-receptor docking protocol with "Induced Fit Refinement" approach.

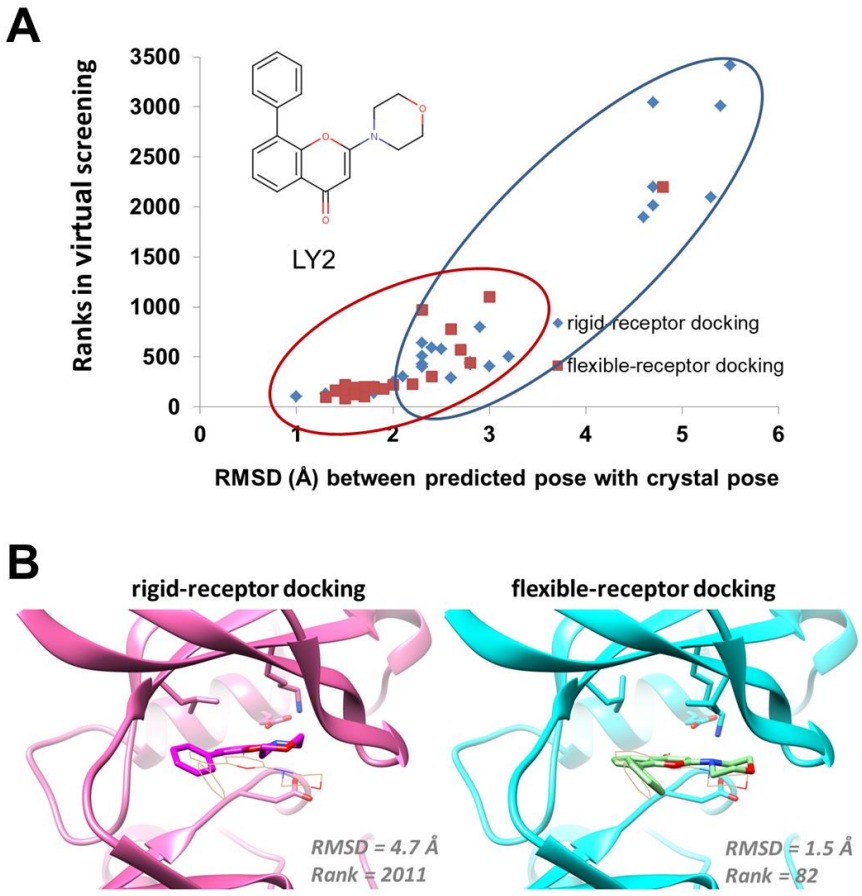

Figure S5. The improved enrichment performance of flexible-receptor docking protocol largely relies on its ability to predict the native-like binding poses. (A) Correlation of binding pose prediction and enrichment performance in Pim-1 kinase, using ligand LY2 as an illustrating example. (B) Comparison of binding poses and virtual screening ranks of LY2 against structure 2BIK by rigid-receptor and flexible-receptor docking protocols.

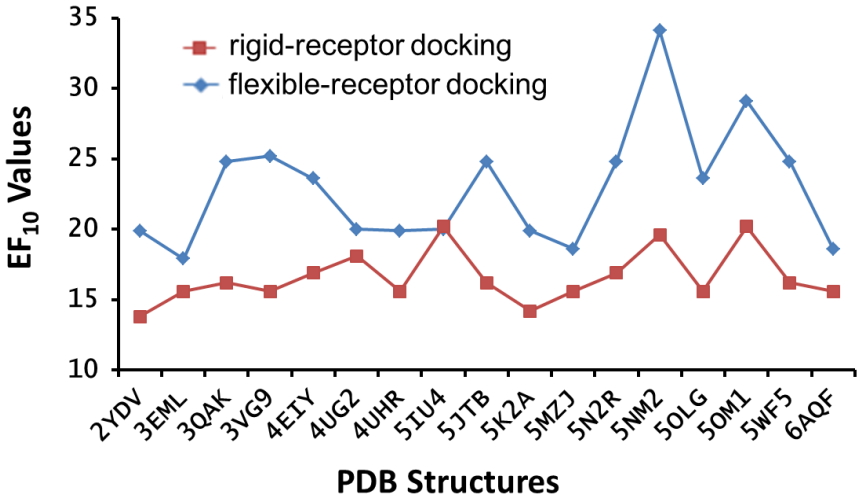

Figure S6. Enrichment performance in retrospective virtual screening of known adenosine A_{2A} ligands.

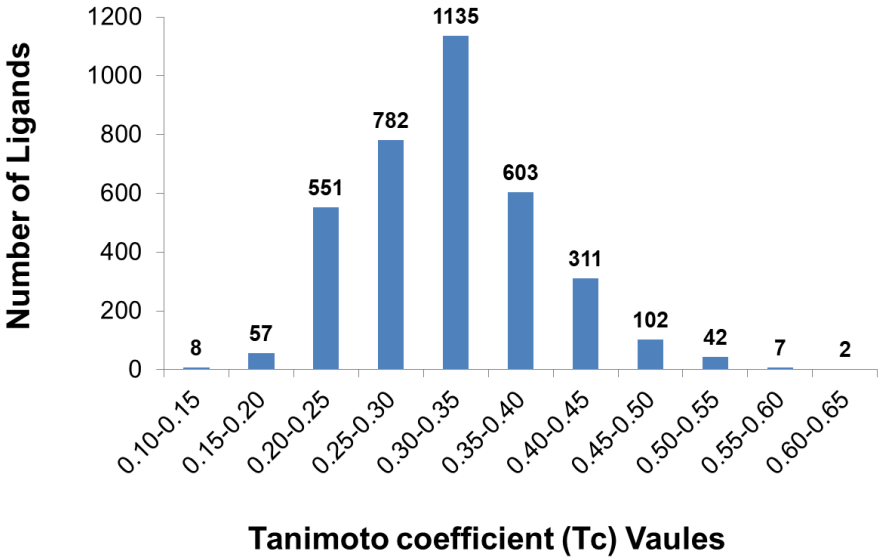

Figure S7. Structural comparison of S26 with known Pim-1 inhibitors in ChEMBL. 3600 known Pim-1 kinase inhibitors from ChEMBL database (with K_i or IC_{50} values better than 1 μM) were compared with S26. The compounds similarities were measured by Tanimoto coefficients (Tc).

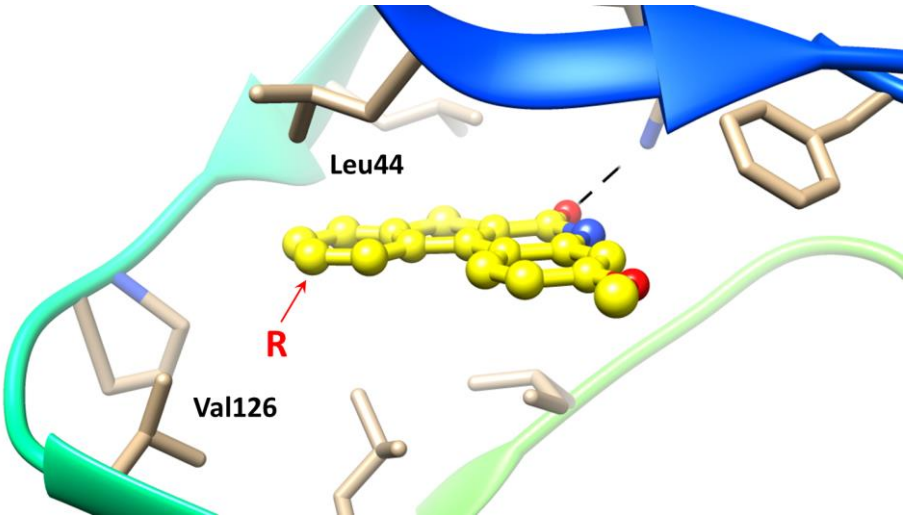

Figure S8. Modifications on S26 to occupy the hydrophobic pocket.

Table S1. Identification of flexible binding-site residues in a diverse target set.

ID	Target	Flexible binding-site residues
1	Pim-1 Kinase	Lys67, Asp186, Glu89, and Leu120
2	A_{2A} receptor	Met270, Tyr271, and Ile274
3	HIV-1 RT	Glu138, Phe227, Trp229, and Tyr188
4	Factor Xa	Tyr99, Phe174, and Gln192
5	Estrogen receptors	Leu346, Met421, Ile424, and His524
6	COX-2	Arg120, His90, and Arg513

Table S2. Selected structurally diverse crystal ligands for cross docking.

ID	Target	Structurally diverse crystal ligands[a]
1	Pim-1 Kinase	01I, 55E, BI1, C4E, IYZ, LI7, LWG, LXG, LY2, LYG, STU, VX1, VX2, VX3.
2	A2A receptor	6DY, 8D1, 9XT, ADN, CFF, CLR, NGI, T4E, UKA, XAC, ZMA.
3	HIV-1 RT	0E8, 1WT, 216, 385, 3OB, 5MA, 65B, AB1, AVX, CXD, DJZ, DMQ, EUR, FTC, G43, GFA, GWB, HBQ, IB1, KBT, M06, M22, NVP, P4Y, PZL, R8D, RT3, S11, TT1, WHU, XK2.
4	Factor Xa	0BN, 0G6, 230, 439, 48U, 4O6, 5QC, 696, 6XS, 701, 894, 931, CBB, CMI, D14, DX9, FFG, FXA, G15, GG2, GSK, H22, I1H, IVK, LGK, OYJ, R11, XMI, YET.
5	Estrogen receptors	0D1, 15Q, 17M, 1GJ, 27G, 29S, 369, 5C4, 5CE, 5DH, 5EU, 5G3, 5HW, 5J2, 5K5, 6WN, 77W, 7EF, 7FD, 85Z, AEJ, DQR, EZT, F3D, FSV, G8Q, G9J, J2Z, KN0, OHT, PIQ, QHG, RAL, VQI, XBR, ZTW.
6	COX-2	416, CEL, D72, DF0 DIF, DXS, FF8, FLP, ICD, LUR, MXM, NPX, T1N.

[a]The ligand labels refer to their ligand ID from the Protein Bank Database (PDB).

Table S3. 14 structurally diverse crystal Pim-1 ligands used for docking.

ID	LIG	Structure	PDB	ID	LIG	Structure	PDB
A	01I	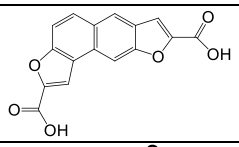	3MA3	**H**	LXG	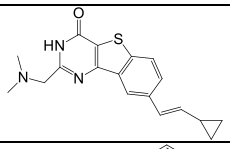	3JXW
B	55E	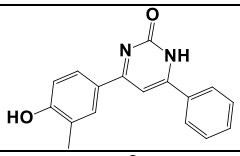	3DCV	**I**	LY2	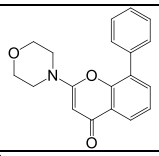	1YI3
C	BI1	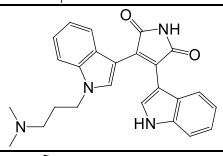	1XWS	**J**	LYG	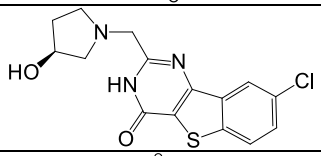	3JY0
D	C4E	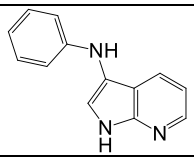	3C4E	**K**	STU	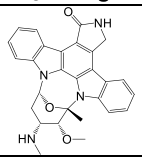	1YHS
E	IYZ	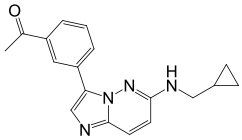	2C3I	**L**	VX1	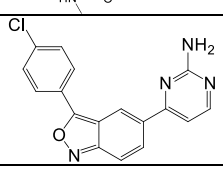	3BGP
F	LI7	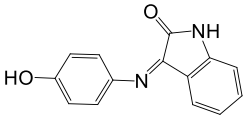	1YXX	**M**	VX2	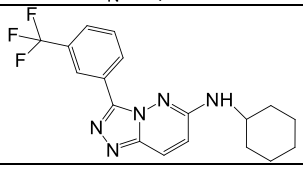	3BGQ
G	LWG	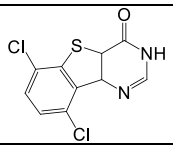	3JYA	**N**	VX3	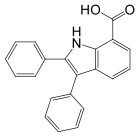	3BGZ

Table S4. 36 Pim-1 PDB structures used for docking.

No.	PDB ID_Chain ID	No.	PDB ID_Chain ID	No.	PDB ID_Chain ID
1	1XQZ_A	**13**	2BIL_B	**25**	3BGZ_A
2	1XR1_A	**14**	2BZK_B	**26**	3C4E_A
3	1XWS_A	**15**	2C3I_B	**27**	3CXW_A
4	1YHS_A	**16**	2J2I_B	**28**	3CY2_A
5	1YI3_A	**17**	2O3P_A	**29**	3CY3_A
6	1YI4_A	**18**	2O63_A	**30**	3DCV_A
7	1YWV_A	**19**	2O64_A	**31**	3F2A_A
8	1YXS_A	**20**	2O65_A	**32**	3JPV_A
9	1YXU_A	**21**	2OBJ_A	**33**	3JXW_A
10	1YXV_A	**22**	3A99_A	**34**	3JY0_A
11	1YXX_A	**23**	3BGP_A	**35**	3JYA_A
12	2BIK_B	**24**	3BGQ_A	**36**	3MA3_A

Table S5. Inhibitory activities against Pim-1 kinase at concentrations of 10 μM and 1 μM.

Structure	Catlog	% Inhibition at 10 μM	% Inhibition at 1 μM
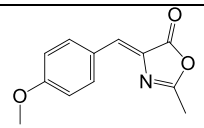	Maybridge PHG00453	7%	-9%
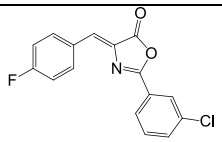	Specs AG-205/32576064	-1%	21%
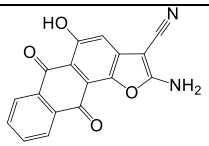	Chemdiv 8010-8291	46%	-10%
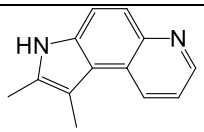	Specs AE-562/12222978	24%	8%
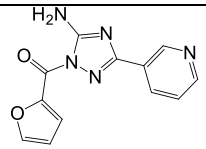	Chemdiv 6855-0473	29%	-6%
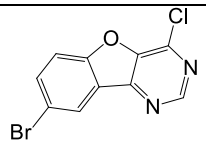	Chemdiv 4353-0017	51%	16%
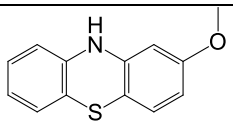	Enamine T5641106	-6%	2%
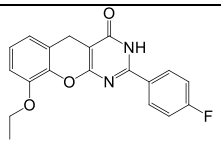	Chemdiv E139-0144	8%	4%
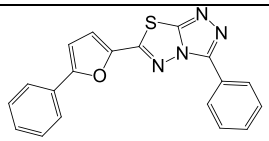	Specs AP-501/43292814	18%	19%
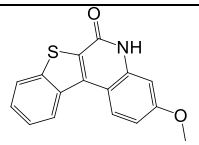	Specs AM-944/40947734 **(S26)**	70%	62%
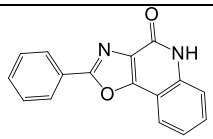	Maybridge BTB11086	17%	15%

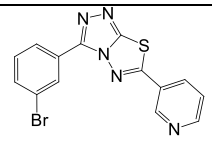	Specs AF-399/43345047	23%	-6%
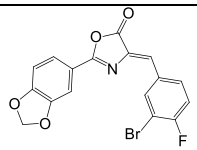	Enamine T6113947	17%	8%
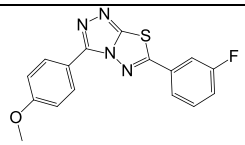	Specs AP-501/43300344	37%	24%
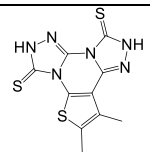	Chemdiv 5586-4259	65%	19%
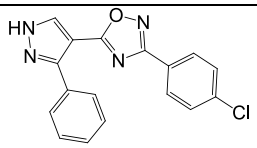	Maybridge CD09386	4%	4%
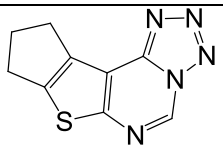	Enamine T0513-8621	36%	6%
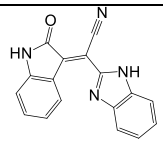	Chemdiv 6186-2756	9%	9%
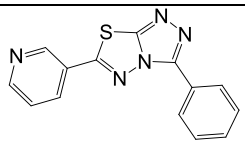	Chemdiv 7009-0145	16%	0%
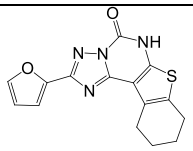	Enamine T6387898	81%	50%
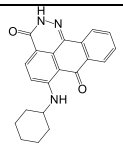	Chemdiv 5451-0533	16%	9%

Table S6. Statistics on data collection and structure refinement.

Data collection	
Space group	P65
Cell dimensions	
a, b, c (Å)	99.37, 99.37, 80.68
α, β, γ (º)	90,90,120
Wavelength (Å)	0.979
Resolution range(Å)[a]	58.86-3.00 (3.16-3.00)
Unique reflections	9182
Redundancy	10.6 (10.9)
I/σ	19.2 (6.3)
Completeness (%)	100 (100)
Structure refinement	
Resolution range (Å)	86.06-3.00 (3.08-3.00)
No. reflections	8724
No. heavy atoms	2203
R_{work}[b]	0.178 (0.233)
R_{free}[c]	0.246 (0.322)
Average B factor (Å^2)	72
Rmsd bond length (Å)	0.014
Rmsd bond angles (º)	1.704
PROCHECK statistics[d]	
Core (%)	93.7
Allowed (%)	5.5
Generally Allowed (%)	0.8
Disallowed (%)	0

[a] Values in parentheses are for the data in the highest resolution shell

[b] $R_{work} = \sum|Fo - Fc|/\sum Fo$, where Fo and Fc are the observed and calculated structure factor amplitudes.

[c] R_{free} is the same as R_{work}, but calculated on 5% reflections not used in refinement.

[d] Analyzed by PROCHECK

Table S7. Structural comparison of S26 with representative Pim-1 inhibitors.

ID [a]	Structure	Tc [b]	ID	Structure	Tc
LGH-447	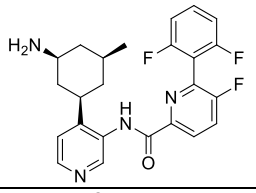	0.22	CX-6258	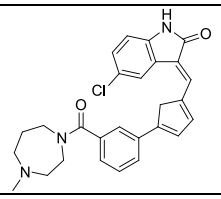	0.19
AZD-1208	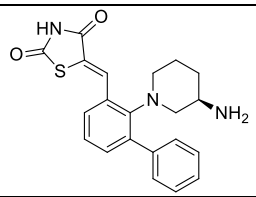	0.23	SMI-4a	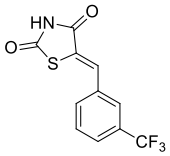	0.2
SGI-1776	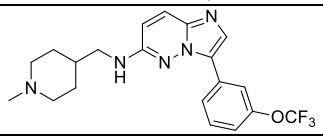	0.26	SEL24-B489	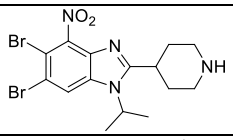	0.19
GEN-955	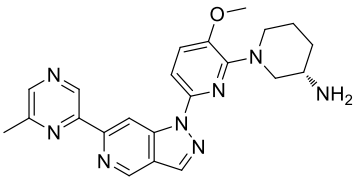	0.29	INCB-053914	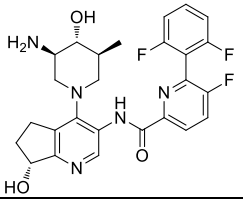	0.26

[a]These Pim-1 inhibitors were advanced into pre-clinical studies or clinical trials.

[b]The compounds similarity were measured by Tanimoto coefficients (Tc).

Experimental Procedures

Computational Methods In general, the flexible receptor docking protocol includes five steps: (1) Analyzing the binding site to identify 3 or 4 flexible residues, which can be done by superimposing all available crystal structures to reflect the conformational changes or by computationally sampling sidechain conformational changes; (2) Based on the concept of "Conformational Selection Model", generating possibly different conformations for each selected residue in the absence of ligand using multi-scale Monte Carlo sampling algorithm, which had been validated in multiple systems before.[1] This is the most time consuming step. However, once the ensemble structures of the residue have been generated, no extra time will be cost in following virtual screening. (3) Clustering the generated multiple conformations for each residue and selecting the representative ones. The representative conformations should cover the majority of the ensemble structures. (4) Subsequently, a flexible-receptor docking algorithm (FlexDock) in DOCK 3.5.54[2, 3] was used to treat these flexible residues independently and recombine them to generate different binding site conformations. (5) Once the protein-ligand complex structures were generated, sidechain conformations of flexible residues were re-built in the presence of docked ligand based on "Induced Fit Model" to generate the final optimized complex structures (FlexRescore). All relevant PDB input files, parameters, scripts and structures used in this manuscrpt are provided in our website (http://www.huanglab.org.cn/zhouyu/flexible-docking/) or GitHub (https://github.com/hnlab/flexible-docking).

1. Preparation of protein and ligand structures.

All crystal structures were retrieved from the Protein Data Bank (PDB). For each PDB strucutre, water molecules were removed. Metal ions were also removed since they were not important for the binding of Pim-1 inhibitors. Protein Local Optimization Program (PLOP)[4-6] was used to add missing hydrogen atoms in protein. Protonation states of His residues were visually inspected by considering the surrounding environment. The ligands were extracted from the PDB structures. The bond orders and formal charges of the ligands were also visually inspected and manually corrected.

2. Generation of multiple conformations for flexible residues

Ligands were removed from holo structures since we wanted to generate all possible conformations for flexible residues without considering the ligand binding effect, which was based on the concept of "Conformational Selection Model". For the selected residues, multi-scale Monte Carlo sampling was used to explore the sidechain flexibility. This method had been comprehensively described elsewhere.[1] Here we would give a brief introduction. The side chain of a single residue was randomly selected from the list of all sampled side chains to generate a reversible trial move and the updated sets of torsions were assigned. In energy calculation, the short-range energy term varied rapidly with respect to the move set, while the long-range energy term varied more slowly. Thus, long-range terms such as electrostatics and the implicit solvent model were updated infrequently, which was called outer loop, while short-range terms such as covalent and local non-bonded interactions were updated at every inner step. This approximation

could facilitate more efficient generation of the complete thermodynamic ensemble. In each simulation, the number of inner loop steps was set as 200 and the number of outer loop steps was set as 15000. The simulation for each selected residue was running parallel at temperature 600 K with 5 rand seeds.

3. Clustering of sidechain conformations.

After the ensemble conformations of each residue were generated, the representative conformations were selected to reduce the number of different conformations used for docking. Firstly, the generated conformations for each residue were ranked by their conformational energies. Secondly, the lowest energy conformation of the residue was picked up and set as cluster one. Thirdly, this lowest energy conformation was compared with the other conformations one by one following the energy rank. Root-mean-square deviations (RMSD) for heavy atoms were calculated to assess the conformational difference. If the RMSD was less than 1 Å, this conformation would be included in cluster one. Otherwise, this conformation was set as cluster two. Fourthly, the lowest energy conformation in cluster two would perform the same conformational comparison as cluster one did. And then cluster three, four, and so on, until all the conformations were put into their clusters. Fifthly, the clusters are re-ranked according to their cluster size since we assumed that the more conformations a cluster contains, the more likely it will be the representative conformation for this residue. Finally, the lowest energy conformations in top-ranked clusters were selected respectively as the representative conformations for the flexible residue.

4. Rigid receptor docking

DOCK 3.5.54 program was used for docking against the ATP binding sites for Pim-1 kinase. Binding site residues were identified as those being within 10 Å of any heavy atom of the co-crystallized ligand. If the crystal structure of Pim-1 was apo structure, it was superimposed onto holo structures to define binding-site residues. The automated docking pipeline was described previously in which all tasks including sphere generation, scoring grid and docking calculations were driven automatically. Receptor-derived spheres were calculated using the program SPHGEN[7] while the ligand-derived spheres were simply generated from the positions of the heavy atoms of the co-crystallized ligand. The matching spheres, required for orientation of the ligand in the binding site, were obtained by augmenting the ligand-derived spheres with receptor-derived spheres, until the total number of spheres was 50. Spheres were labeled for chemical matching based on the hydrogen-bonding properties and charged states of nearby receptor atoms. The grid box dimensions were initially set so that the edges extend 15 Å beyond the matching spheres. Four scoring grids were generated: an excluded volume grid using DISTMAP,[8] a united atom AMBER-based van der Waals potential grid using CHEMGRID,[8] an electrostatic potential grid using DELPHI,[9] and a solvent map using the program SOLVMAP.[10] After rigid-body minimization, ligand-receptor interaction energies were approximated by the sum of electrostatic interaction, van der Waals interaction and ligand desolvation energy.

5. Flexible receptor docking (FlexDock)

A modified version of DOCK 3.5.54 was applied for flexible receptor docking. One different step in our pipeline was that multiple conformations for each flexible residue were generated computationally by multi-scale Monte Carlo sampling. The assumption of FlexDock was that binding site was composed of rigid region and flexible residues, and the flexible residues could move independently. The combination of rigid region and different conformations of flexible residues generated new binding site conformations. The ligand placement algorithm was similar to rigid docking mentioned above except a few modifications. When a ligand adopted some conformations and was placed as some binding modes, a depth-first search was exerted to check whether there was any possibility that it could be accommodated by one generated binding site conformation without generating steric clashes. After that, the roughly accepted ligand binding mode was scored in grids with each independent residue conformation and rigid region. And then the most energy favorable conformation of each flexible residue for this ligand was combined with rigid region to generate the binding site conformation. Since the interaction energy was only calculated between ligand and independent binding site regions respectively, with number of flexible residues increasing, the number of binding site conformations could grow exponentially while the processing time only increased linearly. Each ligand had its own corresponding binding site conformation. One limitation of our pipeline was that the conformational energy of each binding site was not included in final energy estimation, set as 0 for approximation. This energy term will be considered in the further development.

6. Residue side chain rebuilding and rescoring (FlexRescore)

In the step of ligand binding mode determination, the docking tool generated the most favorable receptor conformation for each ligand. In the following step, this generated binding site conformation was further optimized in the presence of ligand based on the concept of "Induced Fit Model". Side chain conformation prediction and minimization for flexible residues were performed using PLOP. The ligands were also minimized while the backbone of flexible residues and all heavy atoms of other residues were fixed.

The binding energy was calculated with a MM-GB/SA method.[11-13] The molecular mechanics forces were divided into short-range components updated frequently, including bond, angle, torsion, and local non-bonded interaction; and long-range components with the long-range forces updated only intermittently. The receptor structure used for initial molecular docking was subjected to energy minimization; the side chain rebuilt protein-ligand complex and the free ligand were also submitted to energy minimization. The binding energy was calculated by subtracting the energies of the optimized free ligand in solvent and the free protein in solvent from the optimized ligand-protein complex's energy in solvent, accounting for protein-ligand interaction energies, desolvation of ligand and protein, and ligand strain energies. The new generated receptor conformations in this step complexed with ligand were ranked by the final binding energy.

Retrospective Evaluation on a Diverse Set of Pharmaceutically Relevant Targets. Here, we performed retrospective evaluation studies for our developed flexible-receptor docking protocol on a diverse set of pharmaceutically relevant targets, which includes Pim-1 kinase, the

adenosine A2A receptor, human immunodeficiency virus type 1 (HIV-1) reverse transcriptase (HIV-RT), factor Xa, estrogen receptors (ER), and cyclooxygenase-2 (COX-2). For the molecular docking studies, structures with diverse conformations of binding-site residues and ligands with diverse chemical structures were selected. The program NMRCLUST,[14] which adopts the KGS-penalty function clustering method,[15] was applied for the conformational clustering of binding-site residues. The program SUBSET, which adopts the fingerprint-based similar analysis method, was applied for the structural clustering of ligands. The docking accuracy was measured by calculating the RMSD between the top scored docking pose and that of the crystallographic ligand. We assessed the quality of the docking screen by the enrichment of annotated ligands of Pim-1 kinase and the adenosine A_{2A} receptor from the vast majority of decoy molecules, which are obtain from DUD. All the protein and ligand structures could be obtained from our website or Github.

Prospective Virtual Screening against Pim-1 Kinase The crystal structure of Pim-1 co-crystallized with ligand LY333531 (PDB ID: 2J2I) was used as receptor model for docking since it had a very unique conformation of which the Lys67 moved away from binding site. In-house compound database containing 200 000 diverse compounds were docked into this receptor model by employing our flexible docking pipeline. All of the compounds in the database were prepared in flexibase format by ZINC pipeline.[16] Based on the analysis of ligand and Pim-1 specific interaction pattern, we defined several structural filters to remove unreasonable docking poses. Firstly, the percentage of ligand heavy atoms contacting with protein heavy atoms shall be greater than 70%. Secondly, the compound shall interact favorably with three apolar residues, including Leu174, Val52 and Ile185. Thirdly, the compound shall form conventional hydrogen bond with backbone carbonyl oxygen of Glu121, unless it forms hydrogen bond interaction with Lys67 or Asp128.

For the ligand similarity comparison, all the reported Pim-1 inhibitors in ChEMBL (with IC_{50} or K_i values better than 1 μM) were collected (last updated in March 2019). Feature key fingerprints were calculated using the default type 2 substructure keys of CACTVS,[17] and the fingerprint-based similarity analysis was performed with the program SUBSET.[18]

Chemistry Compounds S26A and S26B were prepared with reference to the general procedure described in **Scheme S1** (Synthetic Details below). All solvents, chemicals, and reagents were obtained commercially and used without purification. The NMR spectra were obtained in $CDCl_3$, d_6-DMSO, CD_3OD, or d_6-acetone at 25 ℃ at 300 MHz on an OXFORD instrument (Varian), with chemical shift (δ, ppm) reported relative to TMS as an internal standard. HPLC-MS chromatograms and mass spectra were obtained with a Shimadzu LC-MS-2020 system. The prep-HPLC instruments used included a Gilson GX-281(Gilson) and an Elite P230 Preparative Gradient System (Elite). Chiral prep-HPLC was performed with the Elite P230 Preparative Gradient System using Thar Prep-80 and Thar SFC X-5 columns. The microwave instrument used was a CEM Discover SP. All tested compounds had a purity > 95%.

Pim-1 Kinase Assay The activity of Pim-1 kinase was assessed using radiolabeled ATP, which was performed in Reaction Biology Corporation. Peptide substrate ([KKRNRTLTK]) was

first prepared at 20 μM in freshly base reaction buffer. Pim-1 kinase was delivered into the substrate solution. Then compounds in DMSO were delivered into the kinase reaction mixture by Acoustic technology (Echo550; nanoliter range) and incubated for 20 minutes at room temperature. 10 μM [γ-^{33}P]-ATP was delivered into the reaction mixture to initiate the reaction. After 2 hours incubation at room temperature, reactions were spotted onto P81 ion exchange paper. The kinase activity was detected by filter-binding method.

Crystal Structure Determination The crystal of S26 bound Pim-1 kinase was obtained by soaking. Hanging drop vapor diffusion method was applied to crystallize the apo-Pim-1 by mixing 1 μL of protein (10 mg/mL) solution and 1 μL of well buffer at 291 K. PIM1 crystallized in well buffer containing 0.4 M potassium sodium tartrate tetrahydrate after 7 days. For inhibitor soaking, apo-crystal was transferred to a 2 μL drop of well buffer plus 0.2 mM S26, soaked for 1 h. Then the S26 concentration was further increased to 0.5 mM for soaking overnight. The soaked crystal was cyroprotected by the well buffer plus about 25% (v/v) glycerol. A data set was collected using the Rigaku X-ray generator (Cu Kα, 007HF) with the RAXIS IV++ detector. Diffractions were integrated and scaled by Denzo and Scalepack programs. The structure was solved by molecular replacement in Phaser with the apo PIM1 structure (PDB ID: 1YWV)[19] as search model. Ligand fitting and model adjustment werecarried out in Coot, and the model was refined in Refmac5.[20]

Synthetic Details

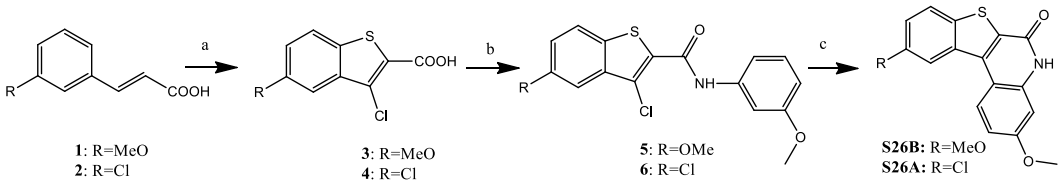

Scheme 1. Synthesis of substituted benzo[b]thieno[2,3-c]quinoline-6(5H)-one-derivatives.

Reagent and conditions: (a) i):SOCl2,4-DMAP,n-hexane,85℃;ii):KOH,methanol/H_2O,80℃. (b)m-Anisidine,EDCI,DCM,rt. (c) hv,(500 W),acetone,4h,rt.

The synthetic procedure of substituted benzo[b]thieno[2,3-c]quinoline-6(5H)-one-derivatives(7,8) was depicted in scheme 1 according to the reported literature.[21] The starting materials were 3-substituted cinnamic acids **1** and **2**, which were commercially available. The corresponding 3-chloro-benzo[b]thiophene-2-carbonyacids **3** and **4** were prepared via two steps, which were the ring-closing reaction by the action of thionyl[22] and hydrolysis reaction of acyl chloride. Carboxamide products **5** and **6** were easily afforded in moderate yield by effecting **3** and **4** in dichloromethane with m-Anisidine through carbodiimide hydrochloride as dehydrating agent. Photochemical dehydrohalogen reaction of intermediates **5** and **6** was accomplished through being irritated by high pressure mercury lamp of 500 W to provide target products S26B and S26A.

General procedure for the synthesis of intermediates 3-chloro-benzo[b]thiophene-2-carbonyacids 3 and 4

A solution of the corresponding 3-substituted cinnamic acids **1** or **2** (1 eq.) in n-hexane was added dropwise thionyl carefully at 55 ℃ over 15 min. The mixture was stirred at 85 ℃ until the start material was completed .The solvent was concentrated under high vacuum through rotary evaporator. The residue was dissolved in the mixed solvent(water and methanol) before KOH (5 eq.) was added to the solution. The mixture was stirred at 80℃ for 6 h. After this time ,diluted hydrochloric acid was used to acidify the solution . Ethyl acetate was added to extract the mixture several times. The combined organic layer was washed with brine, dried over Na_2SO_4 and concentrated under reduced pressure. The intermediates were got for further step without purification.

General procedure for the synthesis of intermediates substituted 3-chloro-benzo[b]thiophene-2-carboxamides 5 and 6

Intermediate **3** or **4** (1 eq.) was dissolved in dichloromethane. m-Anisidine(1.2 eq.) and DMAP (0.1 eq.) were added to the solution. EDCI (1.5 eq.) was added in batches while maintaining the temperature at rt. The mixture was stirred at rt for 2 h. The solvent was removed

under vacuum .The residue was recrystallized with ethyl acetate and petroleum ether to give the title substance.

3-Chloro-5-methoxy-N-(3-methoxyphenyl)benzo[b]thiophene-2-carboxamide (5).

Yielding 86%; Yellow solid. ^{1}H NMR (400 MHz, DMSO d_6) d (ppm): 10.72 (s, 1H),7.73-6.72 (m, 6H),3.99 (s, 3H) ,3.76 (s, 3H). Analytical data are in agreement with those reported elsewhere.[23]

3, 5-dichloro -N-(3-methoxyphenyl)benzo[b]thiophene-2-carboxamide(6)

Yielding 78%; white solid. ^{1}H NMR (400 MHz, DMSO d_6) d (ppm): 10.59 (s, 1H), 8.23-8.21 (d, 0.2H), 7.96-7.94 (d, 1H),7.79-7.77 (d, 0.7H),7.69-7.65 (m, 1H), 7.40 (s, 1H), 7.30-7.29 (d, 1H), 6.76-6.74(d, 2H) ,3.76 (s, 3H)

General procedure for the synthesis of substituted benzothieno[2, 3-c]quinolin-6(5H)-ones 7and 8

Triethylamine (1 eq.)was added to the solution of substituted 3-chloro- benzo[b]thiophene-2-carboxamide **5** or **6** (1 eq.) in acetone at rt. The stirred mixture was irritate by high pressure mercury lamp (500 W) for 4h while the solid was appearing. The precipitate was got by filtration and washed with water and acetone in sequence. The title compounds were afforded by drying in good yields.

3, 10-dimethoxy[l]benzothieno[2,3-c]quinolin-6(5H)-one (S26B)

Yielding 57%; white solid; ^{1}H NMR (400 MHz, DMSO d_6) d (ppm): 12.07 (s, 1H),8.60-8.58 (d, 2H),8.13-8.04 (m, 2H),7.33-7.30 (d, 1H),7.06 (s, 1H), 7.02-7.00 (d, 2H), 3.97 (s, 3H), 3.86 (s, 2H); ^{13}C NMR (100 MHz, DMSO-d_6) d (ppm):159.81, 158.66, 158.38, 139.86, 136.84, 136.27, 134.14, 131.02, 125.36, 125.29, 117.63, 112.02, 111.31, 108.51, 100.29, 56.21, 55.78; MS (ESI^+) m/z for $C_{17}H_{13}NO_3S$ $(M+H)^+$ calcd: 312.07, found: 312.11.

3-methoxy-10-chloro[l]benzothieno[2, 3-c]quinolin-6(5H)-one (S26A)

Yielding 64%; white solid; ^{1}H NMR (400 MHz, DMSO d_6) d (ppm): 12.07 (s, 1H),8.60-8.58 (d, 2H),8.13-8.04 (m, 2H),7.33-7.30 (d, 1H),7.06 (s, 1H), 7.02-7.00 (d, 2H), 3.97 (s, 3H), 3.86 (s, 2H); ^{13}C NMR (100 MHz, DMSO-d_6) d (ppm): 159.71, 158.03, 140.00, 139.57, 136.57, 135.51, 131.01, 127.61, 125.80, 125.20, 124.80, 111.14, 99.86, 55.42; MS (ESI^+) m/z for $C_{16}H_{10}ClNO_2S$ $(M+H)^+$ calcd: 316.02, found: 316.04.

Compounds Characterization

Compound S26A

^{1}H NMR

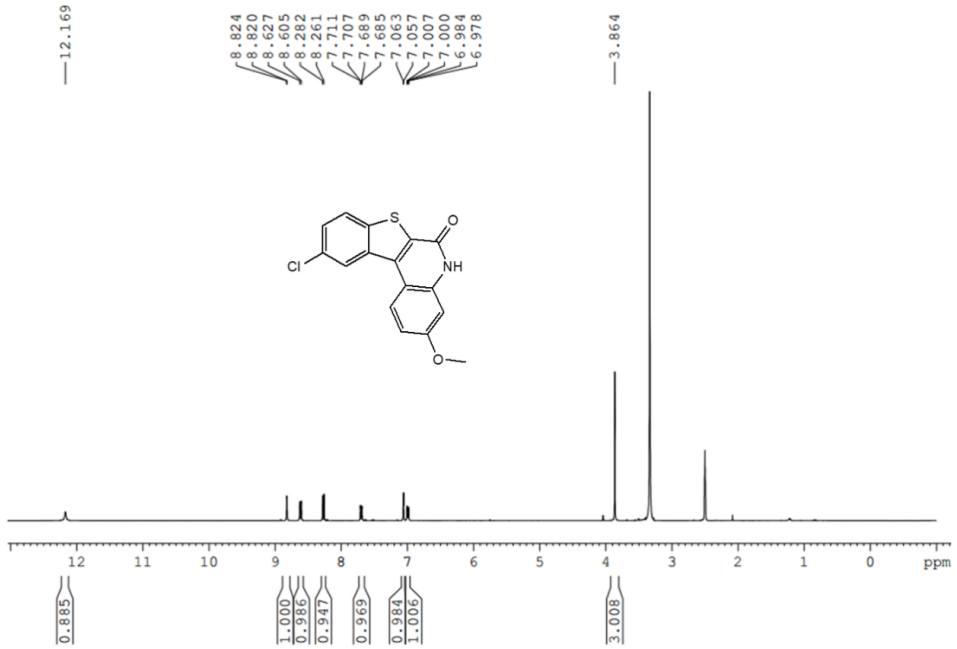

^{13}C NMR

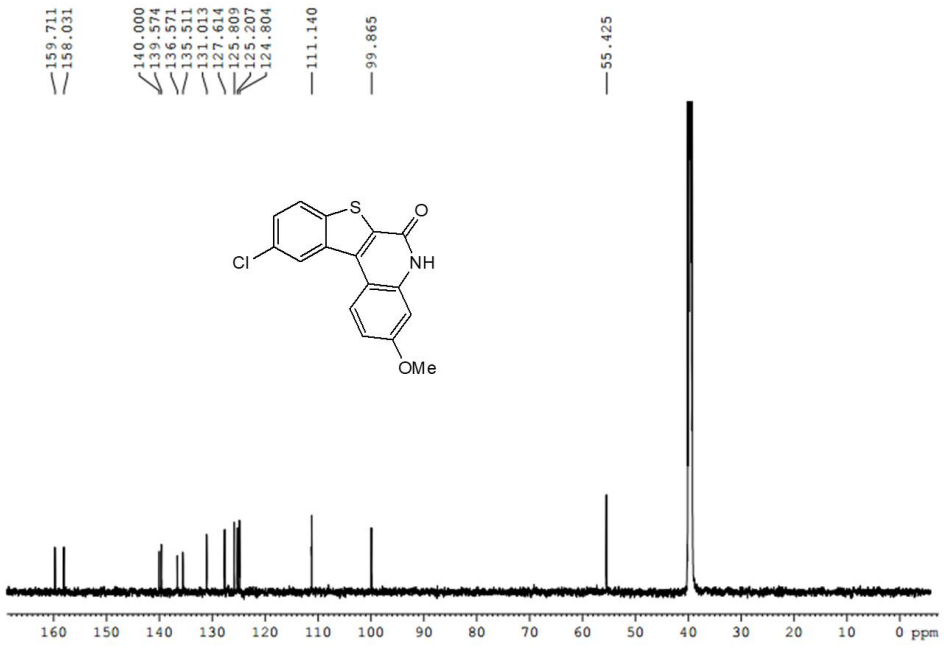

MS(ES^+)

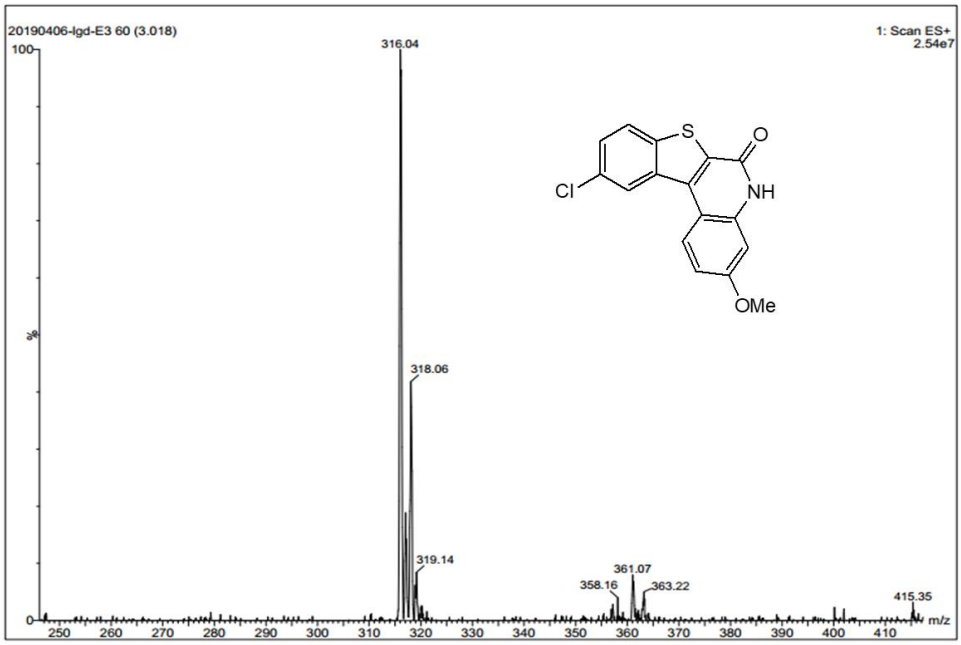
20190406-lgd-E3 60 (3.018)
1: Scan ES+
2.54e7
100
%
0
316.04
318.06
319.14
358.16
361.07
363.22
415.35
250 260 270 280 290 300 310 320 330 340 350 360 370 380 390 400 410
m/z
S
O
Cl
NH
OMe

Compound S26B

^{1}H NMR

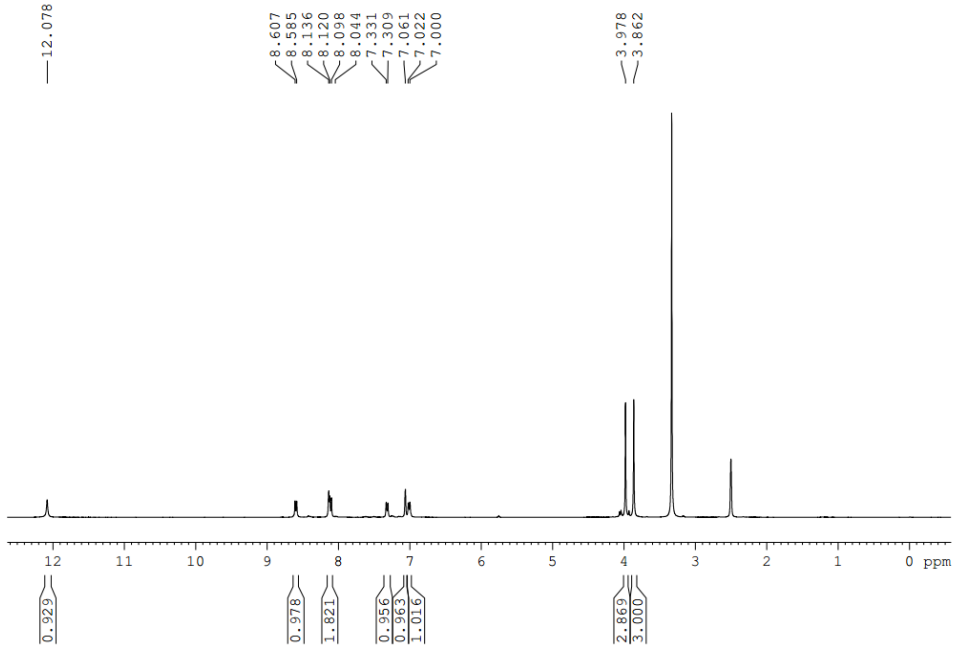

^{13}C NMR

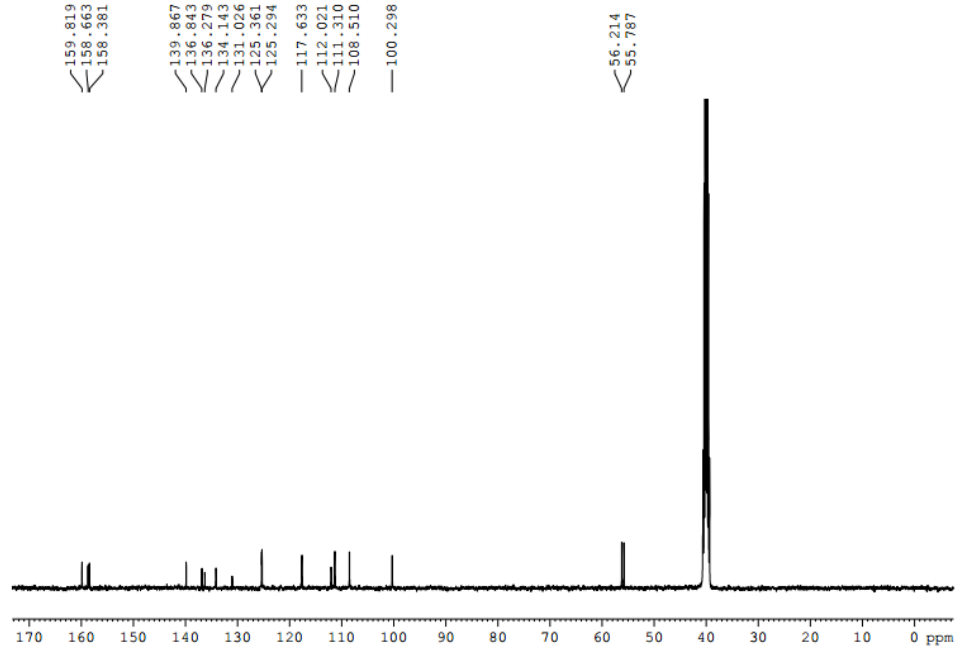

MS(ES^+)

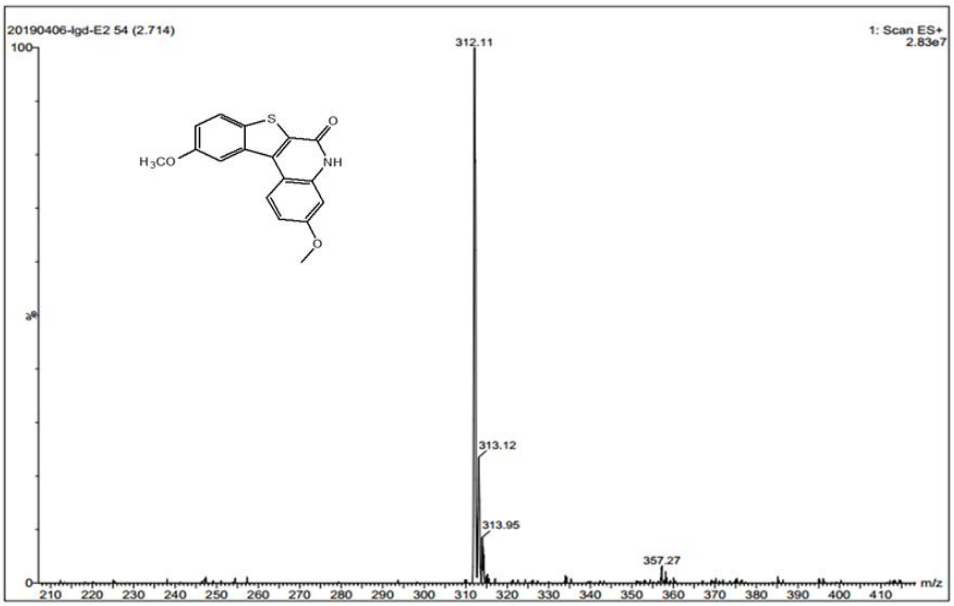
20190406-lgd-E2 54 (2.714)
1: Scan ES+
2.83e7
100
%
0
312.11
313.12
313.95
357.27
210 220 230 240 250 260 270 280 290 300 310 320 330 340 350 360 370 380 390 400 410
m/z
S
O
NH
H3CO
O

References

(1) Nilmeier, J.; Jacobson, M. Multiscale Monte Carlo Sampling of Protein Sidechains: Application to Binding Pocket Flexibility. *J. Chem. Theory Comput.* **2008,** *4*, 835-846.

(2) Wei, B. Q.; Baase, W. A.; Weaver, L. H.; Matthews, B. W.; Shoichet, B. K. A Model Binding Site for Testing Scoring Functions in Molecular Docking. *J. Mol. Biol.* **2002,** *322*, 339-355.

(3) Lorber, D. M.; Shoichet, B. K. Hierarchical Docking of Databases of Multiple Ligand Conformations. *Curr. Top. Med. Chem.* **2005,** *5*, 739-749.

(4) Jacobson, M. P.; Kaminski, G. A.; Friesner, R. A.; Rapp, C. S. Force Field Validation Using Protein Side Chain Prediction. *J. Phys. Chem. B* **2002,** *106*, 11673-11680.

(5) Jacobson, M. P.; Pincus, D. L.; Rapp, C. S.; Day, T. J.; Honig, B.; Shaw, D. E.; Friesner, R. A. A Hierarchical Approach to All-Atom Protein Loop Prediction. *Proteins* **2004,** *55*, 351-367.

(6) Li, X.; Jacobson, M. P.; Friesner, R. A. High-Resolution Prediction of Protein Helix Positions and Orientations. *Proteins* **2004,** *55*, 368-382.

(7) Kuntz, I. D.; Blaney, J. M.; Oatley, S. J.; Langridge, R.; Ferrin, T. E. A Geometric Approach to Macromolecule-Ligand Interactions. *J. Mol. Biol.* **1982,** *161*, 269-288.

(8) Meng, E. C.; Shoichet, B. K.; Kuntz, I. D. Automated Docking with Grid-Based Energy Evaluation. *J. Comput. Chem.* **1992,** *13*, 505-524.

(9) Nicholls, A.; Honig, B. A Rapid Finite Difference Algorithm, Utilizing Successive Over-Relaxation to Solve the Poisson–Boltzmann Equation. *Journal of Comput. Chem.* **1991,** *12*, 435-445.

(10) Mysinger, M. M.; Shoichet, B. K. Rapid Context-Dependent Ligand Desolvation in Molecular Docking. *J. Chem. Inf. Model* **2010,** *50*, 1561-1573.

(11) Huang, N.; Kalyanaraman, C.; Bernacki, K.; Jacobson, M. P. Molecular Mechanics Methods for Predicting Protein-Ligand Binding. *Phys. Chem. Chem. Phys.* **2006,** *8*, 5166-5177.

(12) Huang, N.; Kalyanaraman, C.; Irwin, J. J.; Jacobson, M. P. Physics-Based Scoring of Protein-Ligand Complexes: Enrichment of Known Inhibitors in Large-Scale Virtual Screening. *J. Chem. Inf. Model.* **2006,** *46*, 243-253.

(13) Zhu, K.; Shirts, M. R.; Friesner, R. A. Improved Methods for Side Chain and Loop Predictions via the Protein Local Optimization Program: Variable Dielectric Model for Implicitly Improving the Treatment of Polarization Effects. *J. Chem. Theory Comput.* **2007,** *3*, 2108-2119.

(14) Kelley, L. A.; Gardner, S. P.; Sutcliffe, M. J. An Automated Approach for Clustering an Ensemble of NMR-Derived Protein Structures into Conformationally Related Subfamilies. *Protein Eng. Des. Sel.* **1996,** *9*, 1063-1065.

(15) Peng, S.-M.; Zhou, Y.; Huang, N. Improving the Accuracy of Pose Prediction in Molecular Docking via Structural Filtering and Conformational Clustering. *Chin. Chem. Lett.* **2013,** *24*, 1001-1004.

(16) Irwin, J. J.; Sterling, T.; Mysinger, M. M.; Bolstad, E. S.; Coleman, R. G. ZINC: a FreeTool to Discover Chemistry for Biology. *J. Chem. Inf. Model* **2012,** *52*, 1757-1768.

(17) Ihlenfeldt, W. D.; Takahashi, Y.; Abe, H.; Sasaki, S.-i. Computation and Management of Chemical Properties in CACTVS: An Extensible Networked Approach toward Modularity and Compatibility. *J. Chem. Inf. Comput. Sci.* **1994,** *34*, 109-116.

(18) Voigt, J. H.; Bienfait, B.; Wang, S.; Nicklaus, M. C. Comparison of the NCI Open Database with Seven Large Chemical Structural Databases. *J. Chem. Inf. Comput. Sci.* **2001,** *41*, 702-712.

(19) Kumar, A.; Mandiyan, V.; Suzuki, Y.; Zhang, C.; Rice, J.; Tsai, J.; Artis, D. R.; Ibrahim, P.; Bremer, R. Crystal Structures of Proto-Oncogene Kinase Pim1: a Target of Aberrant Somatic Hypermutations in Diffuse Large Cell Lymphoma. *J. Mol. Biol.* **2005,** *348*, 183-193.

(20) Murshudov, G. N.; Vagin, A. A.; Dodson, E. J. Refinement of Macromolecular Structures by the Maximum-Likelihood Method. *Acta Crystallogr., Sect D: Biol. Crystallogr.* **1997,** *53*, 240-255.

(21) Liscio, P.; Carotti, A.; Asciutti, S.; Ferri, M.; Pires, M. M.; Valloscuro, S.; Ziff, J.; Clark, N. R.; Macchiarulo, A.; Aaronson, S. A. Scaffold Hopping Approach on the Route to Selective Tankyrase Inhibitors. *Eur. J. Med. Chem.* **2014,** *87*, 611-623.

(22) Capek, P.; Zhang, Y.; Barlow, D. J.; Houseknecht, K. L.; Smith, G. R.; Dickerson, T. J. Enhancing the Pharmacokinetic Properties of Botulinum Neurotoxin Serotype A Protease Inhibitors through Rational Design. *ACS Chem. Neurosci.* **2011,** *2*, 288-293.

(23) Pakray, S.; Castle, R. N. The Synthesis of Dimethoxy [1] Benzothieno [2, 3-c] Quinolines. *J. Heterocycl. Chem.* **1986,** *23*, 1571-1577.